SSCL-Preprint-24

SSCL-Preprint-24

Superconducting Super Collider Laboratory

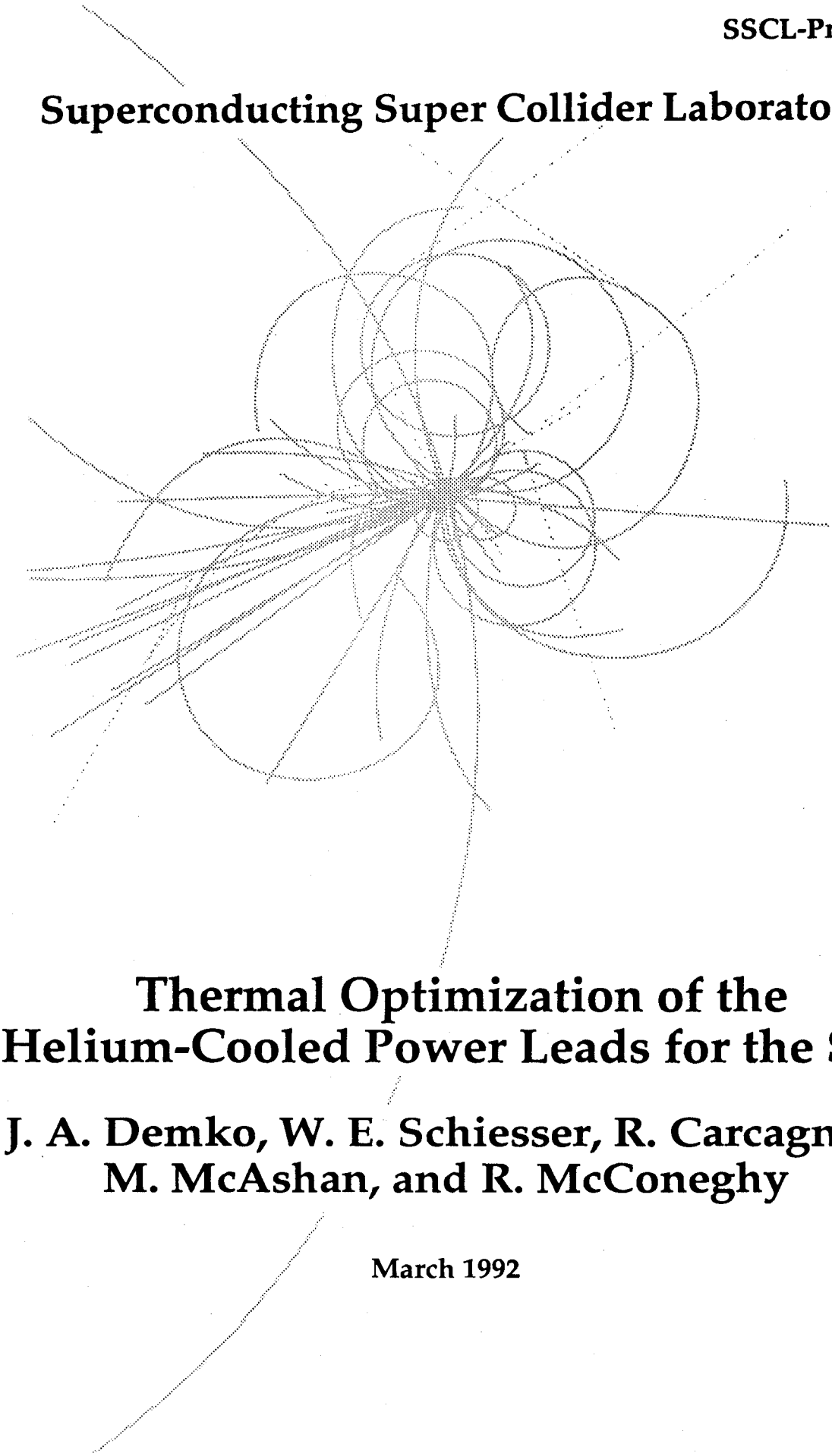

Thermal Optimization of the Helium-Cooled Power Leads for the SSC

J. A. Demko, W. E. Schiesser, R. Carcagno, M. McAshan, and R. McConeghy

March 1992

SSCL-Preprint-24

Thermal Optimization of the Helium-Cooled Power Leads for the SSC*

J. A. Demko, W. E. Schiesser, R. Carcagno,
M. McAshan, and R. McConeghy

Superconducting Super Collider Laboratory†
2550 Beckleymeade Avenue
Dallas, Texas 75237

March 1992

* Presented at the International Industrial Symposium on the Super Collider, New Orleans, March 4–6, 1992.

† Operated by the Universities Research Association, Inc., for the U.S. Department of Energy under Contract No. DE-AC35-89ER40486.

THERMAL OPTIMIZATION OF THE HELIUM-COOLED POWER LEADS FOR THE SSC

J. A. Demko, W. E. Schiesser, R. Carcagno,
M. McAshan, and R. McConeghy

Superconducting Super Collider Laboratory*
2550 Beckleymeade Ave.
Dallas, Texas 75237-3997

INTRODUCTION

The optimum thermal design of the power leads for the Superconducting Super Collider (SSC) will minimize the amount of Carnot work (which is a combination of refrigeration and liquefaction work) required. This optimization can be accomplished by the judicious selection of lead length and diameter. Even though an optimum set of dimensions is found, the final design must satisfy other physical constraints such as maximum allowable heat leak and helium vapor mass flow rate. A set of corresponding lengths and diameters has been determined that meets these requirements for the helium vapor-cooled, spiral-fin power lead design of the SSC.

Early efforts by McFee[1] and Mallon[2] investigated optimizing power leads for cryogenic applications with no convection cooling. Later designs utilized the boiled-off helium vapor to cool the lead. One notable design for currents up to several thousand amps is presented by Efferson[3] based on a series of recommendations discussed by Deiness.[4] Buyanov[5] presents many theoretical models and design formulae but does not demonstrate an approach to thermally optimizing the design of a vapor-cooled lead.

A method for optimizing superconducting magnet current leads is described by Maehata[6] *et al.* The approach assumes that the helium boil-off caused by heat conduction along the power lead into the low-temperature helium is used to cool the lead. The optimum solution is found when the heat flow at the cold end is minimized.

In this study, a detailed numerical thermal model of a power lead design for the SSC has been developed. It was adapted from the dynamic model developed by Schiesser.[7] This model was used to determine the optimum dimensions that minimize the Carnot refrigeration and liquefaction work due to the leads. Since the SSC leads will be cooled by supercritical helium, the flow of vapor is regulated by a control valve. These leads include a superconducting portion at the cold end. All of the material properties in the model are functions of temperature, and for the helium are functions of pressure and temperature. No pressure drop calculations were performed as part of this analysis. The diameter that minimizes the Carnot work was determined for four different lengths at a design current of 6600 amps.

* Operated by Universities Research Association for the U.S. Department of Energy under Contract No. DE-AC35-89ER40486.

POWER LEAD DESCRIPTION

The lead structure is made up of two sections as depicted in Figure 1. The power lead core diameter was varied between 1.2 and 4.0 cm. There are approximately 3.15 fins/cm. The fin thickness and spacing are 0.159 cm. The depth of the spiral fins was held constant at 1.18 cm, providing a constant cross-sectional area of 0.188 cm^2 for the helium flow. An Nb-Ti superconductor cable surrounded by a copper casing is included in the first 30 cm of lead length. The cable has a rectangular cross section given as 0.813 cm × 0.305 cm, resulting in a cross-sectional area for the Nb-Ti of 0.248 cm^2. An assumed copper-to-superconductor ratio for the cable of 1.67 was used in this model. The remainder of the lead core is solid copper. The total length of the lead was varied over 60 cm, 80 cm, 100 cm, and 120 cm—not including the end hardware used to connect to the power supply or to the cryogenic device. The whole lead is convective-cooled by liquid helium that enters at 4K at a pressure of 4 atm. The cooling passages spiral around the outside of the core, removing heat from the lead.

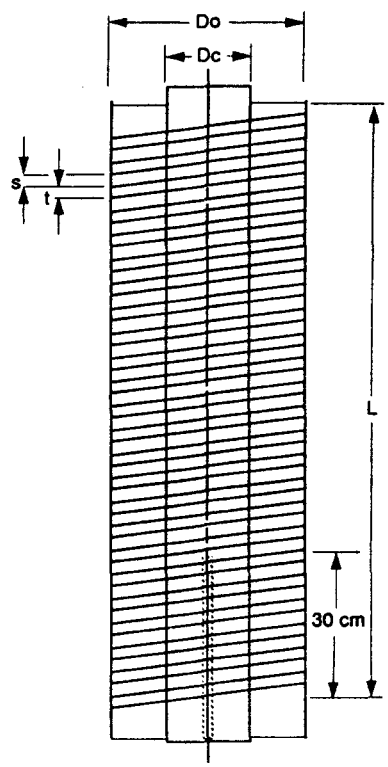

Figure 1. Spiral-Fin, Helium-Cooled Power Lead Design.

MODELING EQUATIONS

The power lead transient thermal analysis was modeled by applying an energy balance to the solid conductor and the helium. These equations are for the solid:

$$\frac{\partial}{\partial t}(\rho_c e_c dv) = \frac{\partial}{\partial x}\left(kA\frac{\partial T_c}{\partial x}\right)dx + h_{\text{conv}}P(T_c - T_v)dx + Q_j \tag{1}$$

and for the helium:

$$\frac{\partial}{\partial t}(\rho_v e_v dv) = \dot{m}\frac{\partial h_v}{\partial s}ds + h_{\text{conv}}P(T_v - T_c)dx. \tag{2}$$

In these equations, e_c and e_v represent the internal energy of the conductor and the helium vapor, respectively, ρ_c and ρ_v refer to the density of the conductor and helium vapor, h_v is the helium vapor enthalpy, h_{conv} is the convective heat transfer coefficient, P is the convection surface area per unit length of the lead, m is the helium mass flowrate, and T_v and T_c are the helium and conductor temperatures, respectively. The quantities dv, dx, and ds are the differential conductor volume, differential distance measured along the axis of the lead, and the differential distance measured along the flow path of the helium, respectively, for which the energy balance is written. The joule heating is determined from the following relation:

$$Q_j = \frac{\rho_{\text{elec}} I^2}{A_{\text{elec}}} dx, \tag{3}$$

where the quantities ρ_{elec} and A_{elec} refer to the electrical resistivity of the lead and the cross-sectional area for electrical conduction. The first term of the right-hand side of the helium energy equation can be written in terms of x using the relation:

$$ds = \Big(1/(\pi \times \text{pitch} \times D)\Big) dx. \tag{4}$$

This formulation can be simplified further. It was determined that the heat capacity of the helium was very small compared to the solid conductor, so it may be neglected. By applying an upwind finite difference technique to the enthalpy derivative, the helium energy equation becomes an algebraic expression for determining the helium liquid temperature.

The heat transfer coefficient is determined from a Dittus-Boelter relation when the flow is turbulent (Re > 2000) given in Wilson,[8] and for laminar flow the Nusselt number based on the aspect ratio of the channel is a constant from Kays.[9] The heat transfer coefficient is given by the following for these two flow regimes:

$$Nu_{\text{laminar}} = \frac{h_{\text{conv}} D_{hyd}}{k_v} = 6.6 \quad \text{and} \tag{5}$$

$$Nu_{\text{turbulent}} = \frac{h_{\text{conv}} D_{hyd}}{k_v} = 0.0259 \times Re^{0.8} \times Pr^{0.4} \times \left(\frac{T_v}{T_c}\right)^{0.716}.$$

In the model, the convection area included two sides of the channel and the channel base. The channel sides were assumed to be isothermal in the radial direction. The resulting algebraic expression becomes:

$$\dot{m}\left(\frac{h_i - h_{i-1}}{\Delta x}\right) = h_{\text{conv}} P (T_c - T_v)_i. \tag{6}$$

The enthalpy term and the convective heat transfer coefficient are evaluated using the conductor temperatures at a given time. This equation can then be used to solve for the new values of the helium vapor temperature along the lead since $h_i = h_i(T_v)$. This approximation is acceptable due to the small difference between the helium and conductor temperatures (usually less than 0.5%), and because the thermal capacitance of the helium is very small in comparison to the lead. Thus the helium temperature changes almost instantaneously with a change in the lead temperature.

The mass flowrate of the helium was determined using a proportional-integral (PI) control algorithm which adjusted the mass flowrate of the helium to maintain the temperature at the top of the lead at a set point of 300K. The equation which describes this is:

$$\dot{m} = \dot{m}_s + K_g \times \left((T - T_{\text{set}}) + \frac{1}{\tau} \times \int_0^{\tau} (T - T_{\text{set}}) dt\right). \tag{7}$$

The second term represents the proportional controller with a gain of $K_g = 0.1$, and the third term is the integral action with a time constant $\tau = 500$ sec. The gain and integral time were set at values for which the dynamic model ran smoothly and efficiently, since only the steady state results were used in the optimization study. This additional ordinary differential equation was integrated as part of the solution to provide the mass flow at each time step.

To solve the resulting system of partial differential equations, the numerical method of lines approach was used as discussed in Schiesser.[10] In this method, the first term on the right-hand side of Eq. (1), which represents the net conduction heat transfer along the lead, was cast into a finite difference form given by:

$$\frac{\partial}{\partial x}\left(kA_c\frac{\partial T_c}{\partial x}\right) = (kA)_{i+\frac{1}{2}}\left(\frac{T_{i+1}-T_i}{\Delta x}\right) - (kA)_{i-\frac{1}{2}}\left(\frac{T_i-T_{i-1}}{\Delta x}\right). \tag{8}$$

The temperature-dependent thermal conductivities at the $i+1/2$ and $i-1/2$ locations were computed based on the geometric mean as recommended by Patankar.[11] The expression for this is:

$$k_{i+\frac{1}{2}} = \frac{2k_{i+1}k_i}{k_{i+1}+k_i}. \tag{9}$$

The lead conduction cross-sectional area is constant except for the prototype lead, which was used to take experimental measurements and had a hollow section at the top. For this case, the area of the hole is simply subtracted from the lead cross section. At the interface region, the proper area is used for the $i+1$ and $i-1$ locations.

The material properties of the conductor were taken for OFHC copper with a residual resistivity ratio (RRR) of 40. The properties of the Nb-Ti superconductor were based on a copper to superconductor ratio of 1.67. Material properties were determined from a database used at the SSC Lab,[12] from Collings,[13] and from Reed and Clark.[14]

Special consideration is also required for the superconducting section in calculating the composite thermal conductivity and the electrical current flow when the superconducting transition occurs in this region. The thermal conductivity of the composite region was based on a simple area-weighted average of the thermal conductivities.

When the Nb-Ti cable is in a superconducting state (*i.e.*, $T < T_{crit}$), it is assumed that the electrical resistivity becomes that of the copper stabilizing the superconductor (based on a copper to superconductor ratio of 1.67) and that all of the current flows through the superconducting cable. The critical temperature was taken to be 10.2K assuming no magnetic field.[14]

At the cold end, a fixed temperature was specified based on measured values. The warm end temperature was controlled to 300K (room temperature), so no heat transfer occurred from the external environment. A convective boundary condition was specified at the warm end of the lead for the comparisons with experimental data. The value of the overall heat transfer coefficient was determined through calibration with the available experimental data. Assuming an environment temperature of 300K, the value of the overall convective heat transfer coefficient was 2.2 W/K. This value was relevant only to the comparisons with experimental measurements since the warm end temperature was 253K. For the initial temperature profile, a linear distribution was specified that ranged from the cold end boundary condition to the desired set point temperature. The current was ramped up at a rate of 6 A/sec until the design current of 6600 A was reached.

Upon making the preceding algebraic substitutions for the spatial derivatives and applying the described boundary conditions, a system of ordinary differential equations in time results. The LSODES integrator was used to solve the resulting system of ordinary differential equations. To ensure that steady state had been reached, the solution was run for a total of 5000 sec.

MODEL VALIDATION

The model validation was based on comparisons with the experimental measurements recently made at Fermilab for the existing prototype lead. The test data were taken on June 19, 1991, for a current of 5007 A. The model used the experimentally measured helium flowrate and end temperatures as inputs. Since the measured top end temperature was below ambient at 253K, it was necessary to calibrate the heat leak into the top end by adjusting a convection coefficient in order to match the measured top temperature at the measured helium flowrate.

The thermal conductivity and electrical resistivity of copper are sensitive to the RRR. Several calibration runs in which the RRR was varied were made to obtain the best fit with the data. Predictions made using RRR = 40 yielded a good fit with the temperature data. Figure 2 shows the temperature distributions along the lead that resulted from the calibration. It is evident from this figure that there is good agreement between the predicted and measured temperatures, particularly near the cold end.

Figure 3 contains comparisons of voltage drop measurements. In order to obtain the best fit with the data, the superconducting transition point was set to match the measured location of $X = 27$ cm. The comparisons show reasonable agreement for $X < 40$ cm. The overall voltage drop across the lead is drastically different (predicted voltage drop is 51 mV, measured 24 mV). Also included in Figure 3 are voltages that were calculated using the experimentally measured temperatures for RRR = 40. These calculated voltages agree fairly well with the model's predictions. The difference is partly due to electrical conduction by the fins, which would reduce the current density. Since there is only one

voltage measurement near the top, an accurate comparison of the voltage distribution is not possible. Additional measurements are being planned to provide better resolution of the voltage distribution along the top half of the lead.

OPTIMIZATION BASIS

The optimum dimensions of the lead were determined by searching for the minimum value of the Carnot work parameter given by:

$$W_{\text{Carnot}} = 7000 \times \dot{m}_{He} + \frac{(T_{TOP} - T_{COLD})}{T_{COLD}} \times Q_{END}. \tag{10}$$

The first term represents the ideal work required to liquefy the helium vapor used to keep the warm end of the lead at room temperature, and it is proportional to the helium mass flowrate. The second term is the ideal refrigeration work required due to heat conduction by the lead at the connection to the cryogenic component (*i.e.*, the cold end of the lead), and it is proportional to the cold end heat conduction. This choice of an optimization parameter is very appropriate for a thermal optimization, since it characterizes the overall system impacts of the power lead design. For the optimization study, a current of 6600 A was assumed for the operating current. The warm end was controlled at 300K. The cold end was assumed to remain at the helium bath temperature of 4K.

RESULTS AND DISCUSSION

Figure 4 shows the Carnot work variation with lead diameter for lead lengths of 60 cm, 80 cm, 100 cm, and 120 cm. In general, the Carnot work decreases as the diameter increases, until a minimum is reached. As the diameter is increased past where the Carnot work minimum occurs, the Carnot work increases sharply. The power leads tend to operate more efficiently at the smaller diameters since the Carnot work is much lower than for the larger diameters. Figure 4 also shows that the optimum power lead diameter increases with increasing total length. The higher values of RRR require smaller diameter leads as well. There is a minimum diameter limit that occurs due to burn-out of the lead if the current density is exceeded. Figure 5 shows the dependence of the mass flowrate of helium on diameter and RRR for the different lengths. The SCDR[15] budget of 0.4 g/sec is exceeded only for the longer leads with small diameters. The flowrate of helium vapor decreases with increasing diameter due to the increased conduction along the lead transferring the heat to the low temperature end and the decreased joule heating along the top end of the lead. The heat transfer conducted along the lead into the cryogenic space is shown in Figure 6. There is no heat conduction for the smaller diameters because of the high flowrate of helium required to remove the heat dissipated at the top. If the diameter were to be decreased further, a condition could be reached where the helium cannot remove the heat generated through dissipation (joule heating) fast enough, and the lead would overheat. As the lead diameter is increased, the heat conduction through the end of the lead increases, which in turn increases the refrigeration load sharply. As the diameter is decreased, the liquefaction load increases due to the increased mass flow of helium required to maintain the top of the lead at the set point temperature of 300K. The minimum Carnot work corresponds to diameters of 1.5 cm, 1.7 cm, 1.9 cm, and 2.0 cm for lengths of 60 cm, 80 cm, 100 cm, and 120 cm, respectively. In Figure 7 a summary of the acceptable design space is shown. The SSC has a conduction heat load limit given as 7.9 W, and a helium mass flow limit of 0.4 g/sec for each lead.[15] The heat transfer constraint requires that the diameter be less than the limit shown in the figure. The mass flow constraint requires that the diameters be greater than the lower mass flow constraint line. Between these constraints lies the locus of diameters that minimize the Carnot work for a given lead length. Since too small a diameter would provide no thermal transient stability, diameters less than 1 cm were not considered.

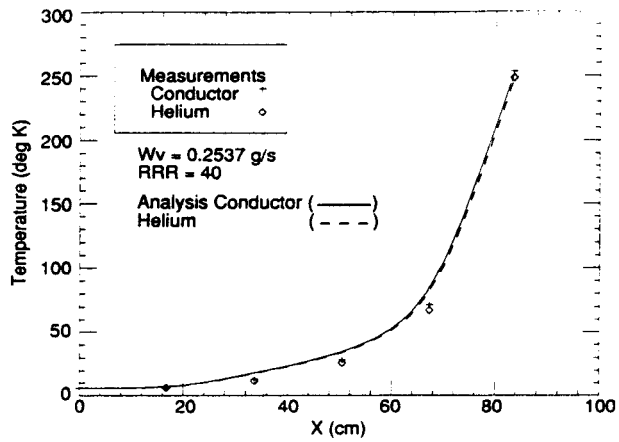

Figure 2. Test Lead Temperature Distributions.

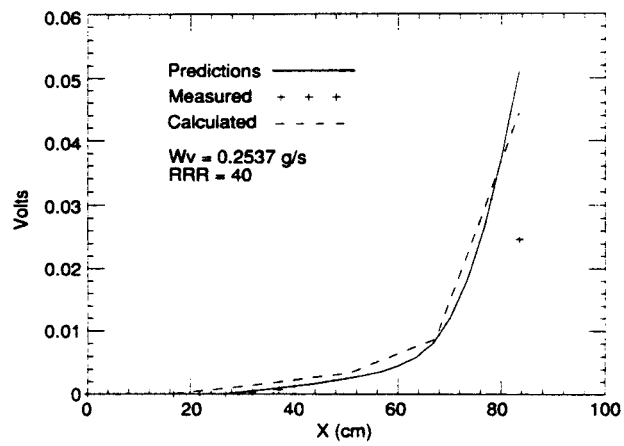

Figure 3. Test Lead Voltage Distributions.

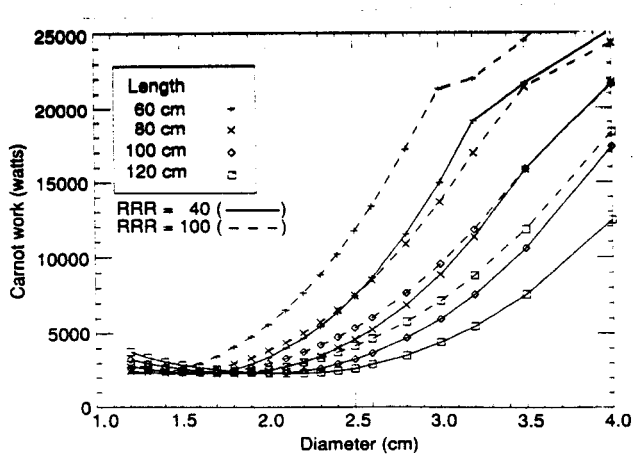

Figure 4. Power Leads Carnot Work.

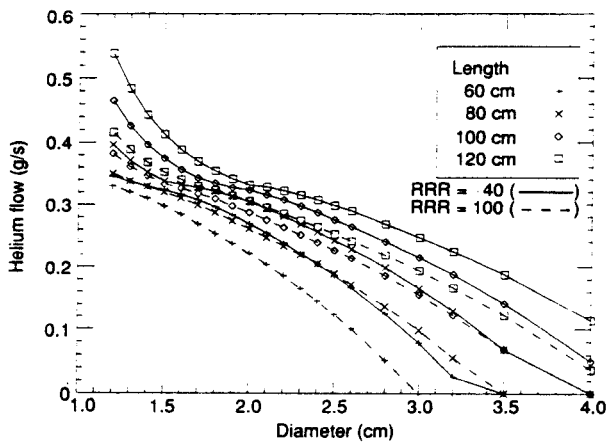

Figure 5. Power Leads Helium Mass Flow.

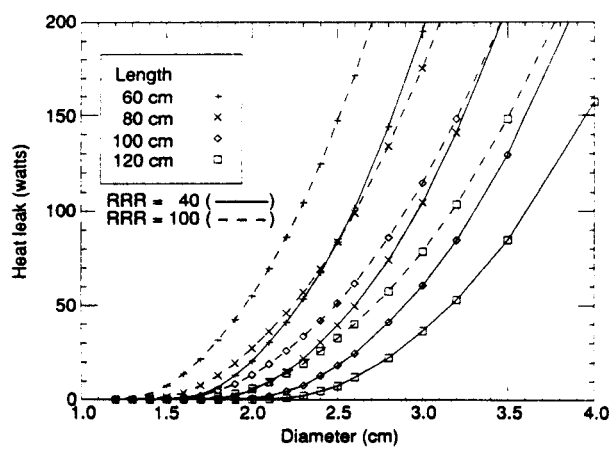

Figure 6. Power Leads Conduction Heat Transfer.

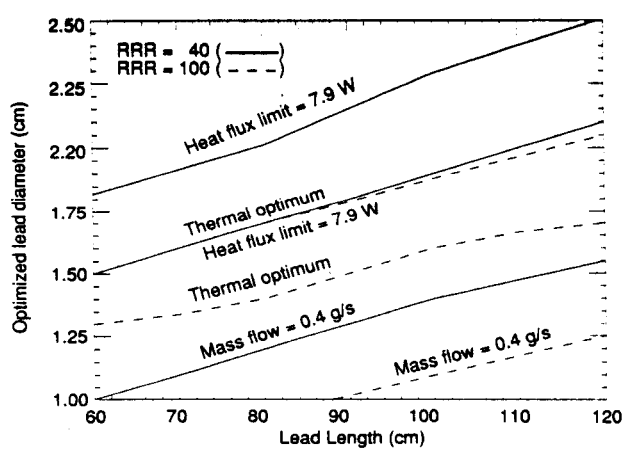

Figure 7. Optimized Power Lead Dimensions.

SUMMARY AND CONCLUSIONS

The thermal model of the spiral fin current lead design has been compared to experimental data with reasonable agreement in temperature and less satisfactory agreement in voltage drop. Comparisons made with voltage drops computed using RRR = 40 and measured temperatures were in agreement with the predicted results. The model has been used to determine the optimum length and diameter for minimizing the ideal Carnot work needed to liquefy the helium vapor used as coolant and to provide refrigeration used to offset the heat leak caused by the connection of the lead to a cryogenic component. Also, the design must meet constraints on heat leak to the cold connection and helium cooling mass flow. The conduction constraint is violated as the diameter is increased beyond some limit for a given length. The mass flow can exceed its constraint if the diameter is too small for a given length. The combination of this information can be used by designers to determine an optimum power lead design for the SSC.

REFERENCES

1. R. McFee, "Optimum Input Leads for Cryogenic Apparatus," *The Review of Scientific Instruments*, **Vol. 30**, No. 2, February 1959.
2. R. G. Mallon, "Optimum Electrical Leads of Aluminum and Sodium for Cryogenic Apparatus," *The Review of Scientific Instruments*, **Vol. 33**, No. 4, April 1962.
3. K. R. Efferson, "Helium Vapor Cooled Current Leads," *The Review of Scientific Instruments*, **Vol. 38**, No. 12, December 1967.
4. S. Deiness, "The Production and Optimization of High Current Leads," *Cryogenics*, **Vol. 5**, October 1965.
5. Yu. L. Buyanov, "Current Leads for Use in Cryogenic Devices. Principle of Design and Formulae for Design Calculations," *Cryogenics*, **Vol. 25**, February 1985.
6. M. Maehata, K. Ishibashi, M. Wake, A. Katase, and M. Kobayashi, "Optimization Method for Superconducting Magnet Current Leads," *Cryogenics*, **Vol. 28**, November 1988.
7. W. E. Schiesser, "A Dynamic Model of the SSC Power Leads," SSC Laboratory Informal Report, August 1990.
8. M. N. Wilson, *Superconducting Magnets*, Clarendon Press, Oxford, 1982.
9. W. M. Kays, *Convective Heat and Mass Transfer*, McGraw-Hill, 1966.
10. W. E. Schiesser, *The Numerical Method of Lines Integration of Partial Differential Equations*, Academic Press, San Diego, 1991.
11. S. V. Patankar, *Numerical Heat Transfer and Fluid Flow*, Hemisphere Publishing Corporation, 1980.
12. A. Devred, SSC Laboratory, Internal Communication.
13. E. W. Collings, *Applied Superconductivity, Metallurgy, and Physics of Titanium Alloys*, Plenum Press, 1986.
14. R. P. Reed, and A. F. Clark, *Materials at Low Temperatures*, American Society for Metals, 1983.
15. J. R. Sanford, and D. M. Matthews, *Site-Specific Conceptual Design of the Superconducting Super Collider*, SSCL-SR-1056, July 1990.